2024-12-09

Enhancements of Heat Islands in the Growing Cities in Developing Countries Due to Land Use Land Cover Changes and Climate Change: A Case of Babati-Tanzania

Majula, Atugonza

Scientific Research Publishing

https://doi.org/10.4236/oje.2024.1412052

Scientific Research Publishing

Open Journal of Ecology, 2024, 14, 891-913
https://www.scirp.org/journal/oje
ISSN Online: 2162-1993
ISSN Print: 2162-1985

Enhancements of Heat Islands in the Growing Cities in Developing Countries Due to Land Use Land Cover Changes and Climate Change: A Case of Babati-Tanzania

Atugonza Sarah Majula*, Revocatus Machunda, Juma Rajabu Selemani

The Nelson Mandela African Institution of Science and Technology, Arusha, Tanzania
Email: *majulaa@nm-aist.ac.tz

How to cite this paper: Majula, A.S., Machunda, R. and Selemani, J.R. (2024) Enhancements of Heat Islands in the Growing Cities in Developing Countries Due to Land Use Land Cover Changes and Climate Change: A Case of Babati-Tanzania. *Open Journal of Ecology*, **14**, 891-913.
https://doi.org/10.4236/oje.2024.1412052

Received: November 1, 2024
Accepted: December 6, 2024
Published: December 9, 2024

Abstract

Climate is changing no doubt, with anthropogenic activities considered as the main driver of the change. Flooding, drought and urban heat island (UHI) are some impacts of climate change (CC). Additionally, land use land cover change (LULCC) adds more pressure to the growing cities. Population is increasing with urban cities expected to accommodate the majority of the people while UHI is expected to increase with CC and LULCC. Adaption is the best option to minimize impacts of UHI; however, researchers are required to identify the cause, impacts and ways to cope with the impacts. Therefore, this study investigated how the Land Surface Temperature (LST) of Babati, a fast-growing town in Tanzania, is changing with CC and LULCC. Remote sensing was used with LULC classification, which was performed using a maximum likelihood algorithm, and LST retrieval involved computational formulas using bands R, NIR, and TIR. Results showed a rise in built-up areas, suggesting urbanization at the expense of farmlands and bare land. The LULCC together with global warming from 2002 to 2022 contributed to the increasing average LST by 0.7˚C signifying that more impacts are expected in the future under a business-as-usual scenario. The findings also indicate that higher vegetation density is associated with lower LST and vice versa. This relationship highlights the critical role of vegetation in regulating temperature and suggests that enhancing vegetation cover may be an effective strategy for mitigating urban heat. Improving agricultural practices as population increases and promoting sustainable urbanization in Babati and similar towns are necessary to mitigate UHI effects.

Keywords

Climate Change, Growing Town, Heat Island, Land Use Land Cover Change,

Land Surface Temperature

1. Introduction

A phenomenon known as "Urban Heat Island" (UHI) occurs when certain places tend to be warmer than their surrounding ones [1]-[3]. Studies [4] [5] show that the absence of vegetation, impermeable surfaces, and human heat are the main causes of the temperature variation. Due to this phenomenon, temperatures in urban residential areas and Central Business Districts (CBD) are higher than those in parks and rural areas.

This phenomenon has a significant negative impact on the environment and the economy including the exacerbation of heat-related illnesses, increased energy consumption, and deterioration of air quality. The impacts of Urban Heat Island (UHI), such as "heat waves," have been extensively demonstrated in numerous studies [6]-[14]. These studies emphasize the importance of conducting researches on a global scale as a means of enhancing living conditions.

Heat waves are among the deadliest recorded hazards in the United States, causing around 131 direct deaths yearly and aggravating underlying health issues [9]. During China's 2018 heat wave crisis, the number of heat-related hospitalizations was at its peak [15] [16], while damage to the sea ecology resulted in significant losses of aquaculture business in Liaoning province. Moreover, UHI has been reported to significantly influence extreme heat in Canada. Both British Columbia and Southern Quebec experienced a heat wave in 2019 and 2010, causing 156 and 280 deaths in eight and five days respectively [10]. Moreover, a study done in India evidenced intense UHI during the day and is projected to intensify if measures are not taken [11]. It is worth noting that areas with intense UHI have shown high Land Surface Temperature (LST).

As a measure of the earth's surface's energy balance and greenhouse gas emissions, LST plays a significant role in modifying the global climate [17] [18]. Higher LST leads to higher energy needs for cooling, which causes greenhouse gas emissions to rise too [19]. The UHI effect is more noticeable in cities because most of the areas are covered by infrastructure such as buildings, roads and pavements that absorb and store more solar radiation, than natural settings. Consequently, it is important to note that changes in the pattern of land use and energy consumption brought about by population growth result in an increasing LST [17] [20]-[23].

A number of studies have assessed the impact of LULC on UHI. A study conducted in Islamabad and Pakistan showed that the UHI effect was found to be greatly exacerbated by a rise in impermeable surfaces, such as roads and buildings [24]. Comparably, a study carried out in Malaysia's Hulu Langat district revealed that urban areas have more LST than rural and forested areas [25]. However, a study by Koko, Yue [26] found that substantial urban expansion with the conversion of

natural surfaces to built-up areas was the cause of the increased mean LST. Population growth has a substantial impact on the link between LULC changes and UHI impacts, making sustainable urban planning necessary to alleviate heat-related difficulties in fast urbanizing locations.

The current global population that resides in cities is approximately 57% [27]. Nearly seven out of ten people will live in cities by 2050, when the urban population is predicted to have more than doubled from its current population. The majority of the growth is expected to occur in low-income, underprivileged nations that rely heavily on nature for their livelihood [28] [29], with sub-Saharan African nations expected to bear the majority of the increase. Rapid population increase has already resulted in many unplanned and uncontrolled communities across Africa [30], posing a constant danger to the continent's ecological and environmental conditions [31]. Despite the fact that most African cities are natural landscapes compared to other continents, the UHI effect persists owing to the separation between impervious surfaces and green spaces [7]. While Göpfert, Wamsler [21] and Pasquini [22] agree on engaging cities and upcoming cities in climate change mitigation and adaptation, it is crucial to consider major urbanization trends that are anticipated to emerge in the upcoming years in order to carry out the Sustainable Development Agenda that includes creating a new urban development framework [27].

Kibassa and Shemdoe [32] and Lindley and Gill [33] emphasized the significance of vegetation, water, and open spaces in creating sustainable and climate-conscious development in urban areas. Cavan, Lindley [30] noted in a study done in two African cities (Addis Ababa and Dar es Salaam) that Africa is projected to have a 1.5 times global mean temperature over the expected increase in global mean temperature due to the fast rate of urban development. Developmental patterns are among other reasons for the temperature rise, as experienced in a study done in Dar es Salaam, Addis Ababa, Khartoum, and Nairobi [34]. Lindley, Gill [35] reported that, there are temperature variations with areas of different characteristics: high temperatures in markets and major roads, while low temperatures in urban parks. Since these effects and magnitude are dependent on climatic conditions and development patterns for that particular location, universal solutions are not entirely consistent. One study conducted in Dar es Salaam and another in Addis Ababa, for example, found that variations in the two cities' spatial patterns contributed to variations in UHI [30].

The Urban Heat Island (UHI) phenomenon is also influenced by the quantity of urban development and its spatial configuration, encompassing factors such as shape, size, arrangement, location, density, dimension, and connectivity [19] [36]. In essence, the way in which urban areas are structured and organized plays a crucial role in shaping the intensity and extent of UHI effects. This understanding underscores the importance of considering not just the scale of urbanization but also its specific characteristics and layout when analyzing and addressing UHI-related challenges. By taking into account the intricate spatial dynamics of urban

environments, policymakers and urban planners can develop more targeted and effective strategies for mitigating the impacts of UHI and promoting sustainable urban development.

Although there have been studies on urbanization and UHI in African cities, there are no such studies for small towns which are experiencing significant uncontrolled population growth while dependent on natural resources [37]. Due to its expected rapid growth, Africa will undoubtedly become the continent with the greatest opportunities and challenges in the twenty-first century, including UHI due to the positive demographic transformation [38]. Therefore, the knowledge of UHI in the context of small towns is of major importance, not only due to uncontrolled population growth but also due to the need to ensure sustainable development by including a comprehensive microclimate analysis [8].

Therefore, this study focuses on Babati town a fast growing town in Tanzania to investigate land use/land cover changes, spatial temperature variations over the past 20 years, and the relationship between land use/land cover and land surface temperature (LST). Due to anthropogenic pressure, Babati's environment has deteriorated, displacing natural landscapes and disrupting ecosystem services [39] [40]. The study will therefore address climate variation concerns in Babati as an emerging city to provide a resource for site-specific LST mitigation techniques.

2. Materials and Methods

2.1. Study Area

Babati Town is an administrative center of the Manyara Region consisting of eight wards: Masaika, Mutuka, Sigino, Bagara, Babati, Nangara, Singe, and Bonga (**Figure 1**), with a total area of 472.9 square kilometres. It lies between 4˚12'39"S and 35˚44'54"E. The town is bordered on all sides by the Babati District, which stretches along Lake Babati and is marked by important trunk road cross-junctions (Arusha, Singida and Dodoma roads).

According to Köppen climate classification [41], Babati has a tropical wet and dry or savanna climate at 1339.09 meters above sea level. The annual mean temperature in the district is 24.89˚C, which is 0.67% higher than the Tanzanian average. The rainfall ranges between 600 mm and 1200 mm annually, with an average annual rainfall of 831, with 131 rainy days (35.95% of the time) [42] [43].

Crop cultivation, livestock keeping, fishing, forestry, mining, quarrying, trade and commerce in the Central Business District, and industrial and tourism activities attract people to migrate, causing rapid urbanization. This has made Babati town among the fastest-growing centers in Tanzania. According to the 2012 household survey by the National Bureau of Statistics (NBS), 58% of the households in Babati town are migrants. The 2022 census report has also indicated that the town's population has grown as expected due to its strategic location and agricultural and economic potential.

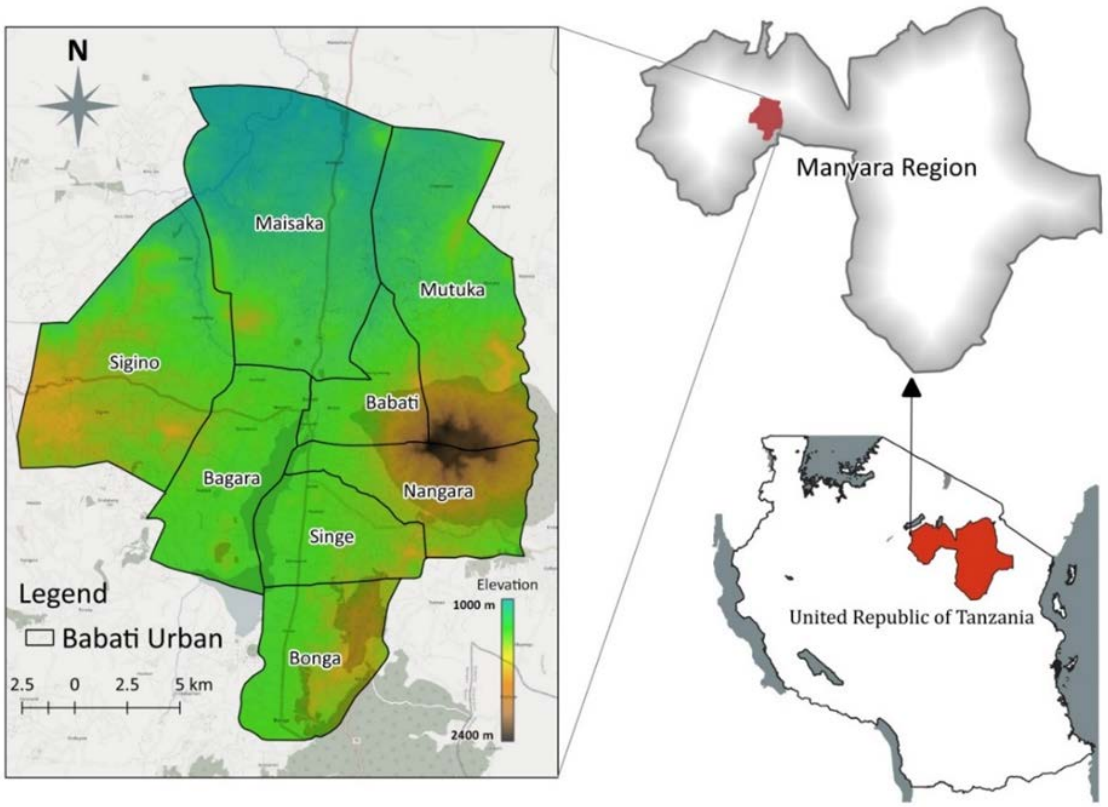

Figure 1. Showing the location of Manyara in Tanzania, location of Babati in Manyara and Babati.

2.2. Assessing Land Use and Land Cover Change (LULCC) of Babati

2.2.1. Data Acquisitions

The study employed three Landsat satellite images from the United States Geological Survey (https://earthexplorer.usgs.gov). They were taken in the dry season when the LST was visible, and there was less than 10% cloud cover. There was a lapse of eleven years and nine years as a result of the poor quality of satellite imagery in 2012. The first image of 2002 was taken from the Landsat 7+ ETM sensor, and the following two images—2013 and 2022—were taken from the Landsat 8 OLI/TIR Table 1.

Table 1. Details of Landsat imagery used.

Sensor	Product ID	Date	Path/Row
Landsat 7 ETM+	LE07_L1TP_168063_20020906_20200916_02_T1	06/09/2002	168/63
Landsat 8 OLI/TIR	LC08_L1TP_168063_20131014_20200912_02_T1	14/10/2013	168/63
Landsat 8 OLI/TIR	LC08_L1TP_168063_20220905_20220914_02_T1	05/09/2022	168/63

The study area was extracted by clipping multiple bands using Babati layer as the mask layer before pre-processing the images for LULC classification and LST

retrieval. Method of data analysis was guided by a specific objective.

2.2.2. Data Analysis

Pre-processing is crucial for minimizing sensor, solar, atmospheric, and topographic distortions in Landsat images [44]. For this study, pre-processing of the images was included for geometric correction, sensor calibration, and sun angle correction. The pre-processed images were clipped and converted to reflectance using Semi-Automatic Classification Plugin (SCP), which detects surface material for each raster using QGIS software. Supervised classification technique was used to create distinct land cover maps for each year. The reflectance images were clipped to create band sets that display different color composites of chosen bands. Followed by using false color composite (FCC) that displays vegetation in shades of red and cyan blue as urban while soils vary from dark to light brown. Training tool in the SCP dock was used to collect training samples that were used to perform classification using the maximum likelihood algorithm. The land covers identified were water, built-up, vegetable, agricultural, and bare land as described in Table 2.

Table 2. Land use land cover classes' description.

Land cover	Description
Water	Rivers, streams, lakes, wetlands, and reservoirs
Built-up	Land occupied by structures constructed by humans, including buildings. Homes, businesses, industrial areas, mixed-use developments, or built-up lands
Vegetation	Together with the predominant cover species, the major vegetation formations, including forest, woodland, shrub land, grassland, and wetland
Agricultural land	Cultivated lands and small shrubs
Bare land	Lands that are less than 10% vegetated and have bare soil, sand, or rocks

The process produced land cover maps for the years 2002, 2013, and 2022, respectively, which were used to assess the relationship between land use and land cover change over the past 20 years.

2.2.3. Accuracy Assessment

Comparing land cover classification to actual data serves as an accuracy assessment, determining how well the classification captures reality. The accuracy was determined using 100 randomly selected pixels for each land cover type and based on visual interpretation and ground truthing. Ground-truthing data came from high-resolution Google Earth and a field visit using GPS [45]. Using the formulas below [46], the information was used to create an error matrix that generated Producer's Accuracy (PA), User's Accuracy (UA), Overall Accuracy, and Kappa values (K).

$$\text{Producer's Accuracy} = \frac{\text{Number of correct classified pixels in each category}}{\text{Number of test set pixels used for that category}} \times 100\% \quad (1)$$

$$\text{User's Accuracy} = \frac{\text{Number of correct classified pixels in each category}}{\text{Number of pixels classified in that category}} \times 100\% \quad (2)$$

$$\text{Overall Accuracy} = \frac{\text{Total number of correct classified pixels}}{\text{Total number of reference pixels}} \times 100\% \quad (3)$$

$$\text{Kappa} = \frac{\text{Observed accuracy} - \text{chance agreement}}{1 - \text{chance agreement}} \quad (4)$$

2.3. Quantifying Urban Heat Island (UHI) over the Years

2.3.1. Land Surface Temperature Estimation for Landsat 7 ETM+

For the year 2002, band 6 image was used starting by converting digital numbers (DN) to radiance using Equation (5), then converting the radiance into brightness temperature (BT) that is in Kelvin with Equation (6). BT in Kelvin was converted in degree Celsius by adding (−273.15) constant as procedures described by [47].

$$L_\lambda = \frac{\text{LMAX}_\lambda - \text{LMIN}_\lambda}{\text{QCALMAX} - \text{QCALMIN}} * (\text{QCAL} - \text{QCALMIN}) + \text{LMIN}_\lambda \quad (5)$$

$$\text{BT} = \frac{K_2}{\ln\left(\frac{K_1}{L_\lambda} + 1\right)} - 273.15 \quad (6)$$

where LMAX and LMIN are spectral values, QCALMAX and QCALMIN are calibration values of pixels while K_1 and K_2 are predetermined constant values, and L_λ is the spectral radiance value of the image. The final result from these algorithms is surface temperature brightness information.

2.3.2. Land Surface Temperature Estimation for Landsat 8 OLI/TIRS

LST retrieval involves computational of a couple of formulas using three bands: R, NIR and TIR [47] [48]. The calculations involved the following procedures.

Conversion to top-of-atmosphere radiance using Equation (7)

$$L_\lambda = M_L \cdot Q_{cal} + A_L \quad (7)$$

L_λ = Top of Atmospheric radiance for wavelength λ (Watts/(m²·srad·μm)), M_L = Band-specific multiplicative rescaling factor, Q_{cal} = Quantized and calibrated standard product pixel values (DN) and A_L = Band-specific additive radiance rescaling factor from the metadata (in the MTL file).

Conversion of the spectral Radiance to At-Sensor Temperature was done using Planck's Law plus (−273.15) to obtain results in Celsius. The spectral radiance was converted to brightness temperature using thermal constants provided in the metadata file using Equation (8),

$$\text{BT} = \frac{K_2}{\ln\left(\frac{K_1}{L_\lambda} + 1\right)} - 273.15 \quad (8)$$

where BT represents Brightness Temperature in degrees Celsius K_1 and K_2 stand for the band-specific thermal conversion constants from the downloaded metadata

and L_λ = TOA spectral radiance (W/(m²·sr·μm)).

Calculation of the NDVI; The NDVI was used to quantify the greenness of vegetation and was suitable for determining vegetation density and detecting changes in plant health. For this reason, the NDVI maps were also extracted to validate LST maps with expected values ranging from +1 to −1. The positive values were representative of healthy green vegetation, while the negative NDVI values indicated non-vegetative cover [49]. In conventional form, NDVI was calculated as a ratio between the red (R) and near infrared (NIR) values using Equation (9) [15]

$$\mathrm{NDVI} = \frac{\mathrm{NIR} - \mathrm{RED}}{\mathrm{NIR} + \mathrm{RED}} \tag{9}$$

whereby, NIR presents reflection in the near-infrared spectrum and RED represents reflection in the red range of the spectrum

Then follows the calculation of the proportion of vegetation (vegetation fraction) P_V, which was used to acquire emissivity using Normalize Difference Vegetation Index (NDVI) values for vegetation and soil, which was estimated using Equation (10).

$$P_V = \left(\frac{\mathrm{NDVI} - \mathrm{NVDI}_{\min}}{\mathrm{NDVI}_{\max} - \mathrm{NDVI}_{\min}} \right) \mathrm{Square} \tag{10}$$

$$\varepsilon = 0.004 * P_V + 0.986 \tag{11}$$

whereby, ε = Land surface Emissivity and P_V = Proportion of vegetation.

All the information was used to estimate Land surface temperature (LST) for Babati town.

$$\mathrm{LST} = \frac{T_b}{1 + \frac{\lambda T_b}{\rho} \ln \varepsilon_\lambda} \tag{12}$$

whereby, LST is Land Surface Temperature, T_b is at-sensor Brightness Temperature (˚C), λ is the wavelength of emitted radiance and ε_λ is the emissivity.

$\rho = h\frac{c}{\sigma}$ where σ is the Boltzmann constant, h is Planck's constant and c is the velocity of light.

The procedure was done for all three imageries to observe the trend and/ or relationship of land surface temperature for the past 20 years from the distribution of land use land cover classes.

2.3.3. UHI Classification

A relative temperature metric was employed to lessen the impact of temperature deviations on long-term analysis, generating four grade maps (**Table 3**) using Equation (13) [50]. Each UHI grade correlates to a specific range of temperature increase, with greater effects as the grade progresses. Understanding these classifications allows urban planners to identify places that require the most intervention and implement effective temperature-management strategies, resulting in

healthier and more sustainable cities.

$$T_R = T/T_{mean} \tag{13}$$

whereby, T_R is relevant temperature, T is the LST and T_{mean} is the average LST value of the map.

UHI Intensity classifying criteria

Table 3. UHI Intensity classification.

T_R	Grade	UHI Intensity
<1.0	1	Green Island
1.0 - 1.1	2	Weak UHI
1.1 - 1.2	3	Moderate UHI
>1.2	4	Strong UHI

2.4. Examining Relationships between LULCC, LST AND NDVI

2.4.1. Correlation between LULC and LST

To examine the effects of LULC types on UHI patterns at the local level, two transects were drawn over the study region. These transects established the LST spatial characteristic of each point across various land cover types along the section profile [51]. The trend link and correlation were established by plotting the findings from several years together and overlaying them.

2.4.2. Correlation between LST and NDVI

Regression analysis between LST and NDVI offers valuable insights into the relationship between vegetation cover and surface temperature. Using GIS software from the System for Automated Geoscientific Analyses (SAGA), the regression equation between Babati town's NDVI and LST was computed. The analysis used LST and NDVI extracted pixels, considering NDVI as the independent variable and LST as the dependent variable, due to the significant influence of vegetation health on LST. The LST and NDVI were found to be adversely associated in a number of studies [52] [53].

3. Results and Discussion

3.1. Accuracy Assessment

Table 4 displays the accuracy assessment for the classified maps. Based on error matrices, the overall accuracy for 2002, 2013, and 2022 was 96.73%, 98.36%, and 99.62%, respectively. While the classified maps' Kappa coefficients were 0.94, 0.96, and 0.99, respectively. These high accuracy rates and Kappa values suggest that the classification methodologies have become more effective over time, likely due to advancements in remote sensing technology and improved algorithms. This consistent enhancement is vital for environmental monitoring and urban planning, as accurate maps are essential for informed decision-making in sustainable land management. Overall, the findings highlight the reliability of the classification

methods and their significance for future research and policy development.

Table 4. Accuracy assessment of the LULC classification of Babati town.

Land use/cover	2002		2013		2022	
	PA	UA	PA	UA	PA	UA
Water	89.32	100	72.70	100	99.25	100
Built up	94.02	95.04	76.40	98.56	98.88	85.63
Vegetation	96.61	98.31	98.61	99.98	99.80	99.12
Farms	99.38	85.25	99.95	97.91	99.62	85.13
Bare land	97.96	97.60	95.67	99.66	93.44	96.64
Overall	96.73		98.36		99.62	
Kappa	0.94		0.96		0.99	

Note: PA—Producer's Accuracy, UA—User's Accuracy.

3.2. Land Use Land Cover Change

LULC maps have been categorized into five classes: Water, Built up, vegetation, agricultural land and bare land (**Figure 2**). For the last 20 years (2002, 2013, 2022), the percentages of classes are as follows: 1.8%, 1.7%, and 1.8% water, 1.2%, 2.1%, and 3.8% built up, 15.1%, 18.4%, and 15.5% vegetation, 78.8%, 76.4%, and 78.3% agricultural land, and 3.2%, 1.4%, and 0.6% bare lands (**Table 5**). LULC maps of Babati town show that farmlands cover the majority of the town in all three figures (years), followed by vegetation and then built-up area. While the built-up area is small compared to other land covers, there has been a significant increase over the 20 years, which went up from 1.2% in 2002 to 3.8% in 2022—a more than three-fold rise.

On top of that trend, the town's economic and social potential is predicted to drive future growth [40]. While the major economic activity is agriculture [40], there has been a decrease in farmland over the years due to the increase of built-up areas near the lake and major truck routes. Despite most studies being conducted in urban settings [11] [15] [19] [30] [32]-[35], Babati has shown similarities in the extension of built-up areas over time. As the population increases, LULC changes displace the natural landscapes and alter the natural systems, including the energy system, resulting in the UHI effect. This is a common trend in many rapidly developing urban areas in developing countries, where the demand for housing and infrastructure development drives urban expansion [34].

Based on the findings, it is anticipated that Babati's natural environment will face significant strain due to expected urban growth, which will have an adverse effect on the ecosystem. In support of this suggestion, Peter, Nnko [39] and Mallya and Rwiza [54] have reported that pressure on the natural environment has already affected public health, energy demand, infrastructure, food security, the economy, and the ecology.

The pattern indicates challenges of dense urbanization in the future, which is linked to environmental deterioration and, as a result, intensifies climate change

concerns through UHI. One of the foreseen effects is a densely urbanized Babati that traps a lot of heat, creating a warm microclimate that, in turn, influences climate change.

A study by Göpfert, Wamsler [21] has recommended that cities should be involved in climate change mitigation; nevertheless, this study emphasizes the significance of including towns too which are future cities in the process. Because small towns are experiencing significant uncontrolled population growth, creating proper LULC change approaches for towns is crucial by involving site-specific mitigation measures. Consequently, adopting sustainable urban development strategies that balance economic growth with environmental protection is critical for sustainable cities.

Table 5. Area percentage and difference of LULCs over the years.

LULC	Area (%) 2002	Area (%) 2013	Area (%) 2022	LULC Change (%) (2002-2013)	LULC Change (%) (2013-2022)	LULC Change (%) (2002-2022)
Water	1.8	1.7	1.8	−0.1	0.1	0.0
Built up	1.2	2.1	3.8	0.9	1.7	2.7
Vegetation	15.1	18.4	15.5	3.3	−2.9	0.4
Farms	78.8	76.4	78.3	−2.4	1.9	−0.5
Bare lands	3.2	1.4	0.6	−1.8	−0.8	−2.6

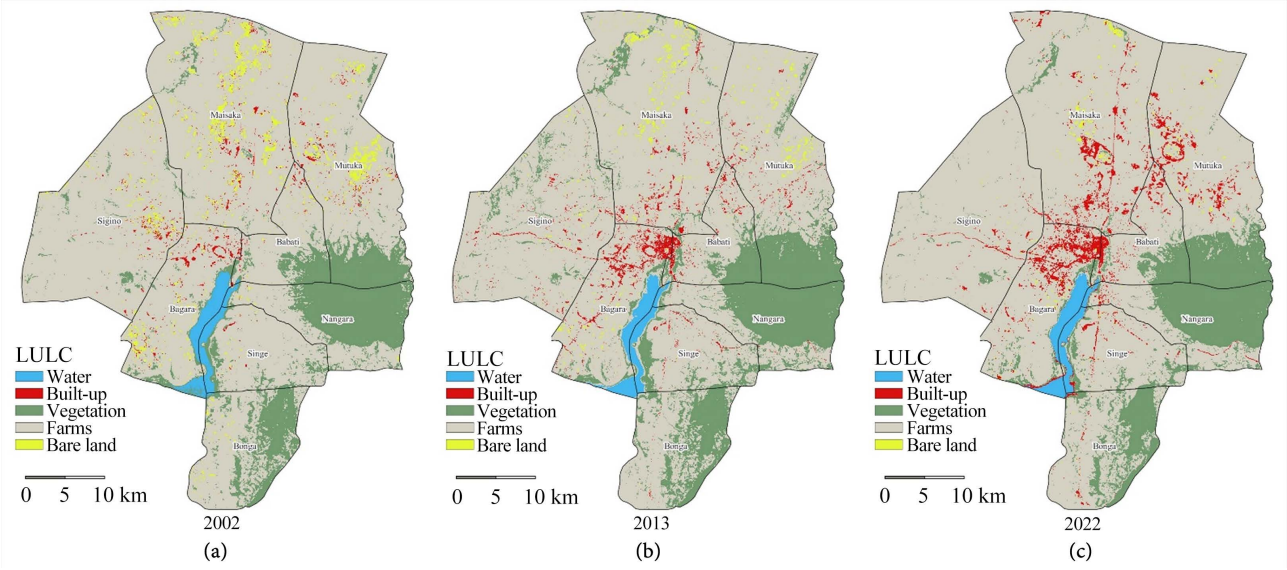

Figure 2. (a) Land use land cover map for year 2002, (b) land use land cover map for year 2013 and (c) land use land cover map for year 2022.

3.3. Spatial NDVI Variation

Figure 3 presents NDVI variations with minimum, maximum and mean of −0.2, 0.70 and 0.25 for the year 2002, −0.64, 0.88 and 0.12 for the year 2013, and −0.50, 0.91 and 0.21, for the year 2022.Water bodies are typically shown by a negative

NDVI, bare land and built-up regions by a positive NDVI of up to 0.2, vegetation by an NDVI of more than 0.2 up to 0.5, and healthier vegetation with a higher chlorophyll content by a higher NDVI of 0.6 and above as shown in **Table 6** [49] [55] [56].

Table 6. NDVI values with the corresponding land cover.

NDVI Value	Different Land Areas
−1 - 0	Water
0 - 0.2	Bare Land and Built-Up Regions
0.2 - 0.5	Vegetation
0.6 - 1	Healthier Vegetation

In 2013, the average NDVI of 0.12 suggests relatively lower vegetation density compared to the other years. Conversely, in 2022, the average NDVI of 0.21 (**Table 7**) indicates a slight improvement in vegetation density compared to 2013.

Table 7. Minimum, maximum and average NDVI values over the years.

Data Used	Min NDVI	Max NDVI	Average NDVI
2002	−0.21	0.70	0.25
2013	−0.64	0.88	0.12
2022	−0.50	0.91	0.21

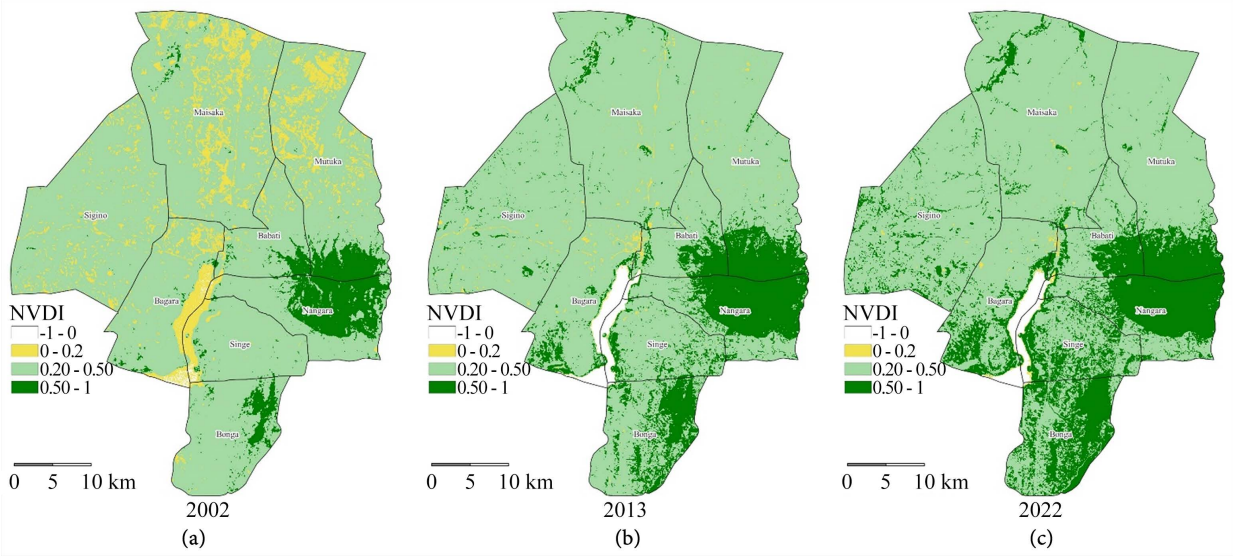

Figure 3. (a) Spatial distribution of NDVI for year 2002, (b) spatial distribution of NDVI for year 2013 and (c) spatial distribution of NDVI for year 2013.

The NDVI data offer important new information about the dynamics of the vegetation in Babati town throughout time. High NDVI values are typically indicated with low LST regions, and vice versa. With this inverse relationship, NDVI maps can be used to validate LST maps. Reducing the amount of energy available

to heat the surface, healthy plants reflect a large portion of incoming sunlight and absorb solar radiation for photosynthesis. Furthermore, the transpiration of water by vegetation results in the latent heat of evaporation, cooling the surrounding air and surface [57]-[59].

Variations in vegetation density can be caused by a variety of factors, including changes in land use, natural disturbances like clearing of natural forests, human activity, specifically in Babati agriculture, and climate variability. These variations are reflected in the NDVI values aligning with studies that suggest ecosystem shifts, including vegetation, as the town expands to accommodate the rapidly growing population [39] [40] [54] [60]. The average NDVI value has decreased over the years, suggesting the interference of natural landscapes as they are transformed into urban areas and agricultural lands. Due to the reason for city expansion, it is expected to have less vegetative cover as the city expands and agriculture activities intensify to accommodate the growing population. This, in turn, will affect the microclimate of the town and ecosystem altogether. In order to better understand all the underlying drivers of vegetation dynamics and to guide land management and conservation strategies in the area, additional study is recommended. This analysis may involve comparing NDVI results with environmental data and field observations.

3.4. Spatial LST Variation

Figure 4 shows LST spatial variations with minimum, maximum, and mean temperatures of 11.2˚C, 39.5˚C, and 25.5˚C in 2002; 10.4˚C, 41.0˚C, and 25.7˚C in 2013; and 15.2˚C, 37.2˚C, and 26.2˚C in 2022 (**Table 8**). Compared to other years, 2013 had the lowest minimum temperature but the highest maximum temperature, and it had the hottest spots. While 2022 has the highest minimum temperature, which is 4˚C higher than 2002, the average temperature is elevated. Temperatures have varied over the years, with lower temperatures (Green Islands) in water and vegetation and higher temperatures (Strong UHI) in some built-up areas and farms/ agricultural lands.

According to the average temperatures, 25.5˚C, 25.7˚C and 26.2˚C for the years 2002, 2013 and 2022 respectively, the study area had high LST (+18˚C). The maps locate a higher percentage of strong UHI in the northern part of Babati, which has less vegetation and water, and a higher percentage of farms/agricultural lands that absorb and store heat from the sun, affecting the surface temperature.

Two transects drawn across the study area analyze in detail the LST characteristic of each point across different land cover types. Although temperatures have varied over time, low temperatures have been observed in water and vegetation and higher temperatures in built-up areas and agricultural lands/farms. This scenario confirms previous research showing that while built-up areas cause hotspots and ultimately lead to UHI, vegetation and water can have cooling effects [32] [51] [61]. Likewise observed is the average LST's upward trend over time, which could be attributed to an increase in anthropogenic activity as the population grows disrupting the natural landscape.

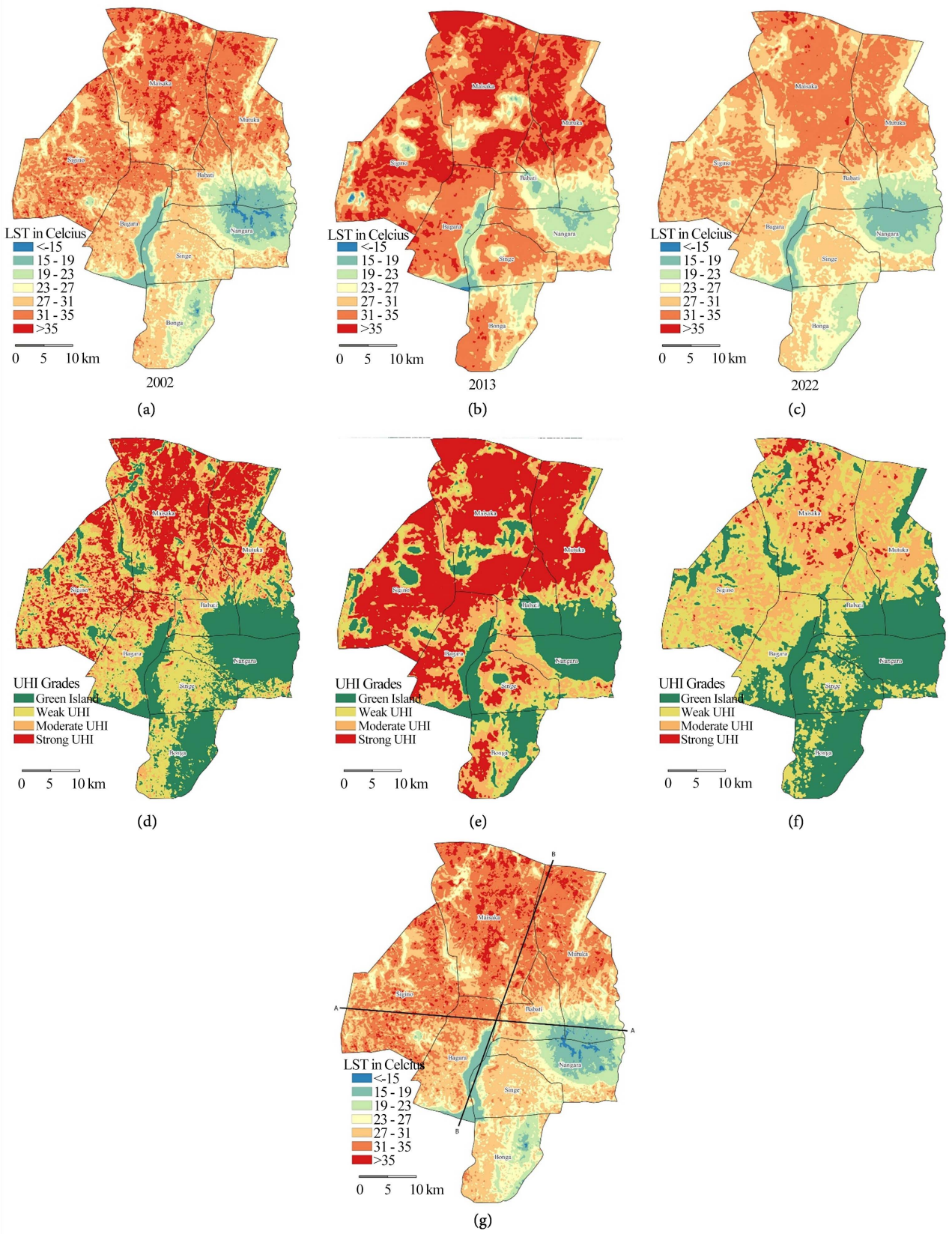

Figure 4. (a) Spatial distribution of LST in 2002, (b) spatial distribution of LST in 2013, (c) spatial distribution of LST in 2022, (d) UHI intensity in 2002, (e) UHI intensity in 2013 and (f) UHI intensity in 2022 and (g) section profile (AA and BB).

Table 8. Land Surface Temperature (LST) variations over 20 years.

Data Used	Min Temperature (˚C)	Max Temperature (˚C)	Average Temperature (˚C)
2002	11.2	39.5	25.5
2013	10.4	41.0	25.7
2022	15.2	37.2	26.2

Despite the fact that built-up areas have appeared as a significant contributor to global warming by having a warmer microclimate [62], this study has identified farmlands as yet another significant source of high temperatures in towns. Contrary to previous research findings, agricultural lands/farmlands are the major LULC contributors to high LST in Babati town. It is quite likely that increased agricultural activity as a result of population growth, which necessitates higher food production, is the primary cause of increasing LST. Higher LST may have resulted from the conversion of natural landscapes into agricultural areas using inadequate techniques [40] that leave the dark loam soil exposed during the dry season [63] [64].

The fact that agricultural activities are a major cultural activity/way of life, the built-up area includes vegetation as a form of urban farming. Integrations of urban farming in built-up areas have made temperatures lower compared to the temperatures in farm/ agricultural lands. The primary explanation for this divergence may be that the analysis's photographs were captured in the dry season, when agricultural lands were cleared to make way for the upcoming rainy season, leaving them barren. Moreover, the characteristics of the exposed dark loam soil is lower albedo which absorbs most of the sun's radiation making it hot. From this observation, it is expected that during cultivation when the earth is covered by crops, these farmlands will have a cool microclimate compared to the dry season.

Given that assessing LST is regarded to be a starting point for evaluating global warming [65], it is crucial to pay attention to agricultural operations as one of the possible principal contributors of high LST. In just 20 years, LST has increased by 0.7˚C.

Despite the fact that farmlands have been the main source of LST, population growth also needs consideration because it has been and is predicted to continue expanding. It is anticipated that the growth will make land more expensive and scarcer, which will eventually prevent the integration of built-up areas and vegetation. Due to the town's economic potential and growing population, a city is anticipated in the near future. This will lead to an increase in anthropogenic activities and the subsequent development of hot spots.

As a result, there is an urgent need to implement sustainable land management practices that reduce the elevated LST effect while also promoting environmental sustainability. Sustainable land use planning practices, such as preserving natural vegetation, promoting low-impact development, and implementing cool roofing and paving materials, can contribute to reducing surface temperatures and improving the overall livability of the town.

3.5. Correlation between LULC and LST

Figure 5 illustrates the spatial distribution of LST across Babati town along transects A-A and B-B, respectively. The variations in LST values provide insights into the thermal characteristics of different land use types within the area. The observed variations in LST values over the years suggest temporal variability in surface temperatures in Babati town. This could be attributed to seasonal changes, land cover dynamics, urbanization processes, and other environmental factors influencing surface heat fluxes.

While there appears to have been some variation in temperature throughout time, places with vegetation cover and water have consistently recorded lower temperatures, indicating the cooling effect of natural elements [52] [53]. Compared to built-up or agricultural land, these areas likely benefit from shading, evaporative cooling, and reduced heat absorption. And elevated temperatures were observed in farmlands, which may be attributed to the exposure of bare soil surfaces to direct solar radiation, limited vegetation cover, and agricultural activities that generate heat.

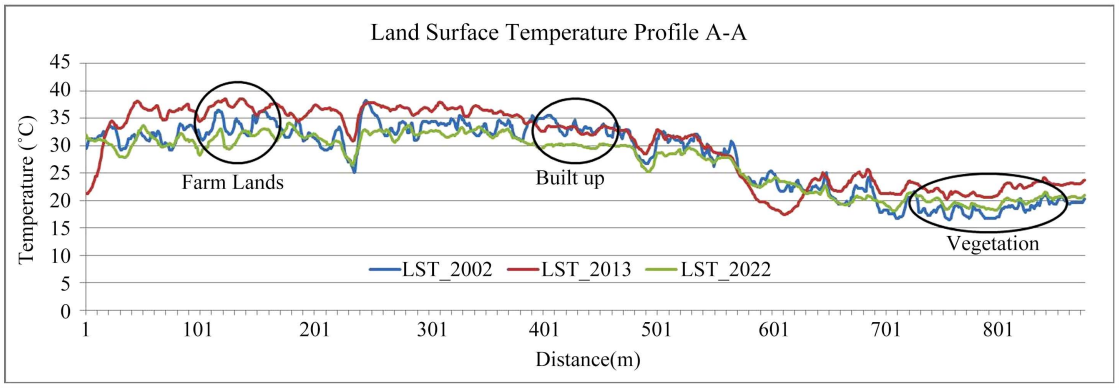

(a)

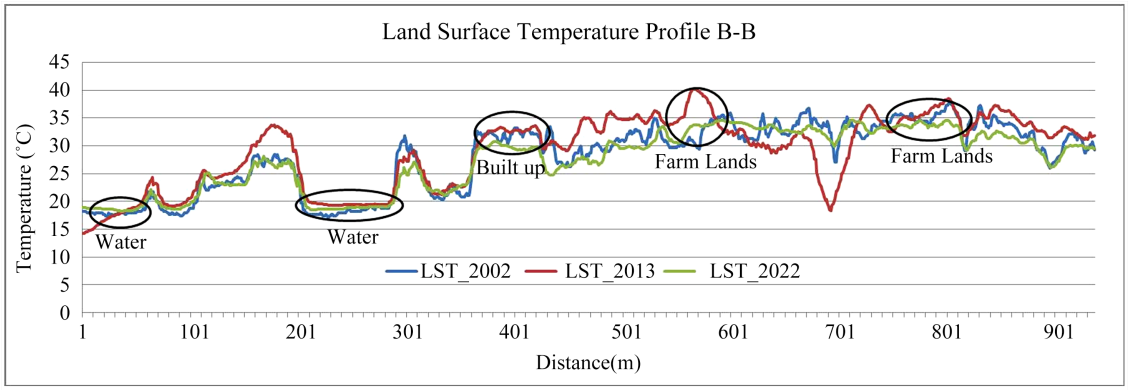

(b)

Figure 5. (a) Section Profile A-A of **Figure 4(d)** and **Figure 4(b)** Section Profile B-B of **Figure 4(g)**.

These results emphasize how crucial it is to maintain natural vegetation and water features when designing metropolitan areas in order to reduce the heat

island effect and encourage cooler temperatures. Furthermore, the findings imply that controlling agricultural practices and establishing more green space are two important aspects of strategic land use planning that can help control surface temperatures and improve the overall thermal comfort of towns and cities.

3.6. Correlation between LST and NDVI

This study found a consistent negative relationship between land surface temperature (LST) and the normalized difference vegetation index (NDVI) in Babati. The correlation was moderately strong in 2002 (−0.76), slightly stronger in 2013 (−0.78), and strong in 2022 (−0.82) (**Figure 6**), indicating that increased vegetation density (NDVI) correlates with decreased surface temperatures (LST). While several studies, such as Khan and Javed [66], have observed a stronger negative correlation with increased moisture content, it is likely that this correlation becomes more pronounced during the wet season, indicating that the negative relationship intensifies as surface moisture increases. The increasingly negative association highlights the importance of preserving and enhancing plant cover to mitigate the urban heat island effect and promote environmental sustainability. The findings provide strong evidence that maintaining and expanding green areas can effectively lower surface temperatures, improving urban climate resilience and livability.

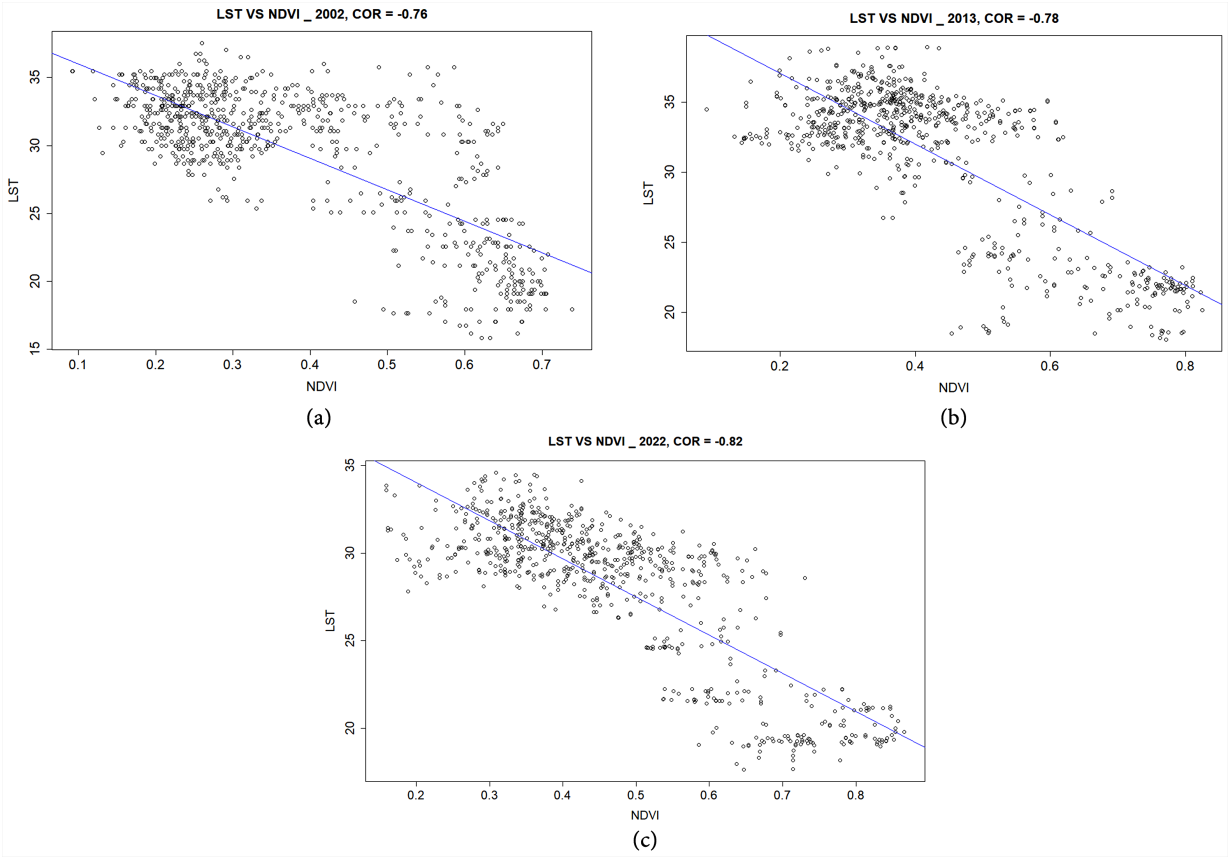

Figure 6. (a) Correlation between LST and NDVI for year 2002, (b) correlation between LST and NDVI for year 2013 and (c) correlation between LST and NDVI for year 2022.

4. Conclusions

Ecosystem and agriculture disruption, heat waves and water scarcity are major challenges of temperature variations. Investing in exploring mitigation strategies in relation to the context as the population grows is crucial to minimizing climate change effects. This study has thoroughly examined the impact of LULC changes on the UHI effect using satellite data, with a focus on the rapidly urbanizing area of Babati, Tanzania. Furthermore, the study establishes the spatial characteristics of vegetation across the region as the major influence of temperature variations.

The results highlight the significant influence of population growth on the increase of built-up areas together with farmlands. As built-up areas increase to accommodate the growing population, agriculture intensifies, too. The population increase has caused disruption of the environment and caused ecosystem shifts. The trend predicts challenges with dense urbanization in the future, which contributes to environmental degradation and, consequently, raises concerns about climate change through urban heat island effects. A heavily urbanized Babati that retains heat and creates a warm microclimate, which in turn affects climate change, is one of the anticipated effects.

Moreover, the study has shown an increase in LST over time and identified farm lands as the major contributing land cover to the increased temperatures. The rapid population growth has resulted in food demands and, in turn, intensification of agricultural activities. The fact that the research was conducted during the dry season, when farmlands are left barren, shows that the dark loam soils have managed to trap heat, making them hot.

The study also demonstrated the cooling effect of vegetation and water across the study area. Surface and ambient air are cooled by the latent heat of evaporation from vegetation's evapotranspiration and water bodies' evaporation. Emphasizing the importance of preserving and integrating vegetation within the study area.

5. Recommendations

The research emphasizes the urgent need for sustainable land use and land cover (LULC) management to combat high land surface temperatures (LST) and promote environmental sustainability, particularly in the context of climate change. As urban areas face rising temperatures and more extreme weather patterns due to climate change, preserving and restoring natural vegetation becomes crucial in mitigating the urban heat island (UHI) effect. Implementing low-impact development strategies, such as green roofs and permeable pavements, helps reduce the environmental footprint of cities while managing stormwater and enhancing cooling. Comprehensive land use planning that prioritizes sustainability and integrates green spaces can reduce reliance on transportation and improve air quality. Furthermore, analyzing the thermal characteristics of various land covers allows for more effective adaptation strategies. By adopting sustainable agricultural practices and establishing monitoring frameworks, urban areas like Babati can build resilience against climate impacts, ultimately improving residents' quality of

life and addressing the challenges posed by a changing climate.

Acknowledgements

Special thanks are extended to Dr. Modest Maurus Baruti, Head of the Department of Landscape Architecture at Ardhi University, for his assistance with the research analysis and for their valuable discussions, which helped to refine the ideas presented in this paper.

Conflicts of Interest

The authors declare that there are no potential conflicts of interest regarding the research, authorship, or publication of this article.

References

[1] Sekertekin, A. and Zadbagher, E. (2021) Simulation of Future Land Surface Temperature Distribution and Evaluating Surface Urban Heat Island Based on Impervious Surface Area. *Ecological Indicators*, **122**, Article 107230. https://doi.org/10.1016/j.ecolind.2020.107230

[2] Dissanayake, D., Morimoto, T., Ranagalage, M. and Murayama, Y. (2019) Land-Use/Land-Cover Changes and Their Impact on Surface Urban Heat Islands: Case Study of Kandy City, Sri Lanka. *Climate*, **7**, 99. https://doi.org/10.3390/cli7080099

[3] Li, D., Liao, W., Rigden, A.J., Liu, X., Wang, D., Malyshev, S., *et al*. (2019) Urban Heat Island: Aerodynamics or Imperviousness? *Science Advances*, **5**, eaau4299. https://doi.org/10.1126/sciadv.aau4299

[4] Ernest, S., Nduganda, A.R. and Kashaigili, J.J. (2017) Urban Climate Analysis with Remote Sensing and Climate Observations: A Case of Morogoro Municipality in Tanzania. *Advances in Remote Sensing*, **6**, 120-131. https://doi.org/10.4236/ars.2017.62009

[5] Wang, H., Zhang, Y., Tsou, J. and Li, Y. (2017) Surface Urban Heat Island Analysis of Shanghai (China) Based on the Change of Land Use and Land Cover. *Sustainability*, **9**, Article 1538. https://doi.org/10.3390/su9091538

[6] Kim, H., Gu, D. and Kim, H.Y. (2018) Effects of Urban Heat Island Mitigation in Various Climate Zones in the United States. *Sustainable Cities and Society*, **41**, 841-852. https://doi.org/10.1016/j.scs.2018.06.021

[7] Kabanda, T.H. and Kabanda, T.A. (2022) Urban Heat Island Analysis in Dar Es Salaam, Tanzania. *South African Journal of Geomatics*, **8**, 98-107. https://doi.org/10.4314/sajg.v8i1.7

[8] Weng, Q., Firozjaei, M.K., Sedighi, A., Kiavarz, M. and Alavipanah, S.K. (2018) Statistical Analysis of Surface Urban Heat Island Intensity Variations: A Case Study of Babol City, Iran. *GI Science & Remote Sensing*, **56**, 576-604. https://doi.org/10.1080/15481603.2018.1548080

[9] Lim, J. and Skidmore, M. (2020) Heat Vulnerability and Heat Island Mitigation in the United States. *Atmosphere*, **11**, Article 558. https://doi.org/10.3390/atmos11060558

[10] Canada, H. (2020) Reducing Urban Heat Islands to Protect Health in Canada. An Introduction for Public Health Professionals. https://www.canada.ca/en/services/health/publications/healthy-living/reducing-urban-heat-islands-protect-health-canada.html

[11] Raj, S., Paul, S.K., Chakraborty, A. and Kuttippurath, J. (2020) Anthropogenic Forcing Exacerbating the Urban Heat Islands in India. *Journal of Environmental Management*, **257**, Article 110006. https://doi.org/10.1016/j.jenvman.2019.110006

[12] Shang, K., Xu, L., Liu, X., Yin, Z., Liu, Z., Li, X., *et al.* (2023) Study of Urban Heat Island Effect in Hangzhou Metropolitan Area Based on SW-TES Algorithm and Image Dichotomous Model. *Sage Open*, **13**, Article 21582440231208851. https://doi.org/10.1177/21582440231208851

[13] Yin, Z., Liu, Z., Liu, X., Zheng, W. and Yin, L. (2023) Urban Heat Islands and Their Effects on Thermal Comfort in the US: New York and New Jersey. *Ecological Indicators*, **154**, Article 110765. https://doi.org/10.1016/j.ecolind.2023.110765

[14] Kiarsi, M., Amiresmaili, M., Mahmoodi, M.R., Farahmandnia, H., Nakhaee, N., Zareiyan, A., *et al.* (2023) Heat Waves and Adaptation: A Global Systematic Review. *Journal of Thermal Biology*, **116**, Article 103588. https://doi.org/10.1016/j.jtherbio.2023.103588

[15] Ren, L., Wang, D., An, N., Ding, S., Yang, K., Freychet, N., *et al.* (2020) Anthropogenic Influences on the Persistent Night-Time Heat Wave in Summer 2018 over Northeast China. *Bulletin of the American Meteorological Society*, **101**, S83-S88. https://doi.org/10.1175/bams-d-19-0152.1

[16] Pan, R., Xie, M., Chen, M., Zhang, Y., Ma, J. and Zhou, J. (2023) The Impact of Heat Waves on the Mortality of Chinese Population: A Systematic Review and Meta-Analysis. *Medicine*, **102**, e33345. https://doi.org/10.1097/md.0000000000033345

[17] Hoornweg, D., *et al.* (2010) Cities and Climate Change: An Urgent Agenda. The World Bank.

[18] Pande, C.B., Egbueri, J.C., Costache, R., Sidek, L.M., Wang, Q., Alshehri, F., *et al.* (2024) Predictive Modeling of Land Surface Temperature (LST) Based on Landsat-8 Satellite Data and Machine Learning Models for Sustainable Development. *Journal of Cleaner Production*, **444**, Article 141035. https://doi.org/10.1016/j.jclepro.2024.141035

[19] Li, X. and Zhou, W. (2019) Optimizing Urban Greenspace Spatial Pattern to Mitigate Urban Heat Island Effects: Extending Understanding from Local to the City Scale. *Urban Forestry & Urban Greening*, **41**, 255-263. https://doi.org/10.1016/j.ufug.2019.04.008

[20] Yang, J., Zhan, Y., Xiao, X., Xia, J.C., Sun, W. and Li, X. (2020) Investigating the Diversity of Land Surface Temperature Characteristics in Different Scale Cities Based on Local Climate Zones. *Urban Climate*, **34**, Article 100700. https://doi.org/10.1016/j.uclim.2020.100700

[21] Göpfert, C., Wamsler, C. and Lang, W. (2018) A Framework for the Joint Institutionalization of Climate Change Mitigation and Adaptation in City Administrations. *Mitigation and Adaptation Strategies for Global Change*, **24**, 1-21. https://doi.org/10.1007/s11027-018-9789-9

[22] Pasquini, L. (2019) The Urban Governance of Climate Change Adaptation in Least-Developed African Countries and in Small Cities: The Engagement of Local Decision-Makers in Dar es Salaam, Tanzania, and Karonga, Malawi. *Climate and Development*, **12**, 408-419. https://doi.org/10.1080/17565529.2019.1632166

[23] Xu, S., Wang, D., Liang, S., Jia, A., Li, R., Wang, Z., *et al.* (2024) A Novel Approach to Estimate Land Surface Temperature from Landsat Top-of-Atmosphere Reflective and Emissive Data Using Transfer-Learning Neural Network. *Science of the Total Environment*, **955**, Article 176783. https://doi.org/10.1016/j.scitotenv.2024.176783

[24] Sadiq Khan, M., Ullah, S., Sun, T., Rehman, A. and Chen, L. (2020) Land-Use/Land-

Cover Changes and Its Contribution to Urban Heat Island: A Case Study of Islamabad, Pakistan. *Sustainability*, **12**, Article 3861. https://doi.org/10.3390/su12093861

[25] Rendana, M., Idris, W.M.R., Rahim, S.A., Abdo, H.G., Almohamad, H., Al Dughairi, A.A., *et al*. (2023) Relationships between Land Use Types and Urban Heat Island Intensity in Hulu Langat District, Selangor, Malaysia. *Ecological Processes*, **12**, Article No. 33. https://doi.org/10.1186/s13717-023-00446-9

[26] Koko, A.F., Yue, W., Abubakar, G.A., Alabsi, A.A.N. and Hamed, R. (2021) Spatiotemporal Influence of Land Use/Land Cover Change Dynamics on Surface Urban Heat Island: A Case Study of Abuja Metropolis, Nigeria. *ISPRS International Journal of Geo-Information*, **10**, 272.

[27] UN (2023) The 2018 Revision of the World Urbanization Prospects. Population Division of the United Nations Department of Economic and Social Affairs (UN DESA).

[28] Maja, M.M. and Ayano, S.F. (2021) The Impact of Population Growth on Natural Resources and Farmers' Capacity to Adapt to Climate Change in Low-Income Countries. *Earth Systems and Environment*, **5**, 271-283. https://doi.org/10.1007/s41748-021-00209-6

[29] Gu, D., Andreev, K. and Dupre, E.M. (2021) Major Trends in Population Growth around the World. *China CDC Weekly*, **3**, 604-613. https://doi.org/10.46234/ccdcw2021.160

[30] Cavan, G., Lindley, S., Jalayer, F., Yeshitela, K., Pauleit, S., Renner, F., *et al*. (2014) Urban Morphological Determinants of Temperature Regulating Ecosystem Services in Two African Cities. *Ecological Indicators*, **42**, 43-57. https://doi.org/10.1016/j.ecolind.2014.01.025

[31] Mubako, S., Nnko, H.J., Peter, K.H. and Msongaleli, B. (2022) Evaluating Historical and Predicted Long-Term Land Use/Land-Cover Change in Dodoma Urban District, Tanzania: 1992-2029. *Physics and Chemistry of the Earth*, *Parts A/B/C*, **128**, Article 103205. https://doi.org/10.1016/j.pce.2022.103205

[32] Kibassa, D. and R, S. (2016) Land Cover Change in Urban Morphological Types of Dar Es Salaam and Its Implication for Green Structures and Ecosystem Services. *Modern Environmental Science and Engineering*, **2**, 171-186. https://doi.org/10.15341/mese(2333-2581)/03.02.2016/005

[33] Lindley, S. and Gill, S. (2013) Green Infrastructure: An Essential Foundation for Sustainable Urban Futures in Africa.

[34] Li, X., Stringer, L.C. and Dallimer, M. (2021) The Spatial and Temporal Characteristics of Urban Heat Island Intensity: Implications for East Africa's Urban Development. *Climate*, **9**, Article 51. https://doi.org/10.3390/cli9040051

[35] Lindley, S.J., Gill, S.E., Cavan, G., Yeshitela, K., Nebebe, A., Woldegerima, T., *et al*. (2015) Green Infrastructure for Climate Adaptation in African Cities. In: *Future City*, Springer, 107-152. https://doi.org/10.1007/978-3-319-03982-4_4

[36] Li, L., Zhan, W., Hu, L., Chakraborty, T., Wang, Z., Fu, P., *et al*. (2023) Divergent Urbanization-Induced Impacts on Global Surface Urban Heat Island Trends since 1980s. *Remote Sensing of Environment*, **295**, Article 113650. https://doi.org/10.1016/j.rse.2023.113650

[37] Chapman, S., Watson, J.E.M., Salazar, A., Thatcher, M. and McAlpine, C.A. (2017) The Impact of Urbanization and Climate Change on Urban Temperatures: A Systematic Review. *Landscape Ecology*, **32**, 1921-1935. https://doi.org/10.1007/s10980-017-0561-4

[38] Grinin, L. and Korotayev, A. (2023) Africa: The Continent of the Future. Challenges

and Opportunities. In: *World-Systems Evolution and Global Futures*, Springer, 225-238. https://doi.org/10.1007/978-3-031-34999-7_13

[39] Peter, K.H., Nnko, H.J. and Mubako, S. (2020) Impacts of Anthropogenic and Climate Variation on Spatiotemporal Pattern of Water Resources: A Case Study of Lake Babati, Tanzania. *Sustainable Water Resources Management*, **6**, Article No. 47. https://doi.org/10.1007/s40899-020-00400-z

[40] Ministry of Lands and URT (2019) Babati Town Master Plan 2017-2037.

[41] Beck, H.E., Zimmermann, N.E., McVicar, T.R., Vergopolan, N., Berg, A. and Wood, E.F. (2018) Present and Future Köppen-Geiger Climate Classification Maps at 1-km Resolution. *Scientific Data*, **5**, Article 180214. https://doi.org/10.1038/sdata.2018.214

[42] Karlsson, M. (2016) Environmentally Friendly Agriculture in Tanzania: A Case Study of a Farm in Himiti Village, Babati.

[43] Venance, S.K., Mshenga, P. and Birachi, E. (2016) Factors Influencing On-Farm Common Bean Profitability: The Case of Small-Holder Bean Farmers in Babati District, Tanzania. *Journal of Economics and Sustainable Development*, **7**.

[44] Young, N.E., Anderson, R.S., Chignell, S.M., Vorster, A.G., Lawrence, R. and Evangelista, P.H. (2017) A Survival Guide to Landsat Preprocessing. *Ecology*, **98**, 920-932. https://doi.org/10.1002/ecy.1730

[45] Larbi, I., *et al*. (2019) Predictive Land Use Change under Business-as-Usual and Afforestation Scenarios in the Vea Catchment, West Africa.

[46] Lillesand, T., Kiefer, R.W. and Chipman, J. (2015) Remote Sensing and Image Interpretation. Wiley.

[47] Tariq, A., Riaz, I., Ahmad, Z., Yang, B., Amin, M., Kausar, R., *et al*. (2019) Land Surface Temperature Relation with Normalized Satellite Indices for the Estimation of Spatio-Temporal Trends in Temperature among Various Land Use Land Cover Classes of an Arid Potohar Region Using Landsat Data. *Environmental Earth Sciences*, **79**, Article No. 40. https://doi.org/10.1007/s12665-019-8766-2

[48] Luan, Y. (2020) Retrieval of Land Surface Temperature from Landsat 8 Data of the Dandong-Liaoyang Geothermal Area.

[49] Guha, S. and Govil, H. (2020) An Assessment on the Relationship between Land Surface Temperature and Normalized Difference Vegetation Index. *Environment, Development and Sustainability*, **23**, 1944-1963. https://doi.org/10.1007/s10668-020-00657-6

[50] Xu, X., Pei, H., Wang, C., Xu, Q., Xie, H., Jin, Y., *et al*. (2023) Long-Term Analysis of the Urban Heat Island Effect Using Multisource Landsat Images Considering Inter-Class Differences in Land Surface Temperature Products. *Science of the Total Environment*, **858**, Article 159777. https://doi.org/10.1016/j.scitotenv.2022.159777

[51] Zhao, Z., He, B., Li, L., Wang, H. and Darko, A. (2017) Profile and Concentric Zonal Analysis of Relationships between Land Use/Land Cover and Land Surface Temperature: Case Study of Shenyang, China. *Energy and Buildings*, **155**, 282-295. https://doi.org/10.1016/j.enbuild.2017.09.046

[52] Grover, A. and Singh, R. (2015) Analysis of Urban Heat Island (UHI) in Relation to Normalized Difference Vegetation Index (NDVI): A Comparative Study of Delhi and Mumbai. *Environments*, **2**, 125-138. https://doi.org/10.3390/environments2020125

[53] Rani, M., Kumar, P., Pandey, P.C., Srivastava, P.K., Chaudhary, B.S., Tomar, V., *et al*. (2018) Multi-Temporal NDVI and Surface Temperature Analysis for Urban Heat Island Inbuilt Surrounding of Sub-Humid Region: A Case Study of Two Geographical Regions. *Remote Sensing Applications: Society and Environment*, **10**, 163-172.

https://doi.org/10.1016/j.rsase.2018.03.007

[54] Mallya, C.L. and Rwiza, M.J. (2021) Influence of Land Use Change on Nitrate Sources and Pollutant Enrichment in Surface and Groundwater of a Growing Urban Area in Tanzania. *Environmental Earth Sciences*, **80**, Article No. 111. https://doi.org/10.1007/s12665-021-09386-z

[55] Choudhury, D., Das, K. and Das, A. (2019) Assessment of Land Use Land Cover Changes and Its Impact on Variations of Land Surface Temperature in Asansol-Durgapur Development Region. *The Egyptian Journal of Remote Sensing and Space Science*, **22**, 203-218. https://doi.org/10.1016/j.ejrs.2018.05.004

[56] Marzban, F., Sodoudi, S. and Preusker, R. (2017) The Influence of Land-Cover Type on the Relationship between NDVI–LST and LST-Tair. *International Journal of Remote Sensing*, **39**, 1377-1398. https://doi.org/10.1080/01431161.2017.1402386

[57] Jiang, Y. and Weng, Q. (2016) Estimation of Hourly and Daily Evapotranspiration and Soil Moisture Using Downscaled LST over Various Urban Surfaces. *GI Science & Remote Sensing*, **54**, 95-117. https://doi.org/10.1080/15481603.2016.1258971

[58] Januar, T.W., Lin, T., Huang, C. and Chang, K. (2020) Modifying an Image Fusion Approach for High Spatiotemporal LST Retrieval in Surface Dryness and Evapotranspiration Estimations. *Remote Sensing*, **12**, Article 498. https://doi.org/10.3390/rs12030498

[59] Xiong, Y., Zhao, S., Yin, J., Li, C. and Qiu, G. (2016) Effects of Evapotranspiration on Regional Land Surface Temperature in an Arid Oasis Based on Thermal Remote Sensing. *IEEE Geoscience and Remote Sensing Letters*, **13**, 1885-1889. https://doi.org/10.1109/lgrs.2016.2616409

[60] Katonge, J.H., Kaswamila, A.L. and Hamisi, M.I. (2019) Impact of Land Use Changes on the Health of Lakes Babati and Burunge, Northern Tanzania. 12*th Tawiri Scientific Conference*, Arusha, 4-6 December 2019.

[61] Simwanda, M., Ranagalage, M., Estoque, R. and Murayama, Y. (2019) Spatial Analysis of Surface Urban Heat Islands in Four Rapidly Growing African Cities. *Remote Sensing*, **11**, Article 1645. https://doi.org/10.3390/rs11141645

[62] Chen, X., Zhao, H., Li, P. and Yin, Z. (2006) Remote Sensing Image-Based Analysis of the Relationship between Urban Heat Island and Land Use/Cover Changes. *Remote Sensing of Environment*, **104**, 133-146. https://doi.org/10.1016/j.rse.2005.11.016

[63] Fayiga, A.O., Ipinmoroti, M.O. and Chirenje, T. (2017) Environmental Pollution in Africa. *Environment, Development and Sustainability*, **2**0, 41-73. https://doi.org/10.1007/s10668-016-9894-4

[64] Xiao, B. and Bowker, M.A. (2020) Moss-Biocrusts Strongly Decrease Soil Surface Albedo, Altering Land-Surface Energy Balance in a Dryland Ecosystem. *Science of the Total Environment*, **741**, Article 140425. https://doi.org/10.1016/j.scitotenv.2020.140425

[65] Bokaie, M., Zarkesh, M.K., Arasteh, P.D. and Hosseini, A. (2016) Assessment of Urban Heat Island Based on the Relationship between Land Surface Temperature and Land Use/Land Cover in Tehran. *Sustainable Cities and Society*, **23**, 94-104. https://doi.org/10.1016/j.scs.2016.03.009

[66] Khan, Z. and Javed, A. (2022) Correlation between Land Surface Temperature (LST) and Normalized Difference Vegetation Index (NDVI) in Wardha Valley Coalfield, Maharashtra, Central India. *Nova Geodesia*, **2**, Article 53. https://doi.org/10.55779/ng2353